

Cluster-liquid transition in finite, saturated fermionic systems

Ebran, Jean-Paul; Khan, E.; Nikšić, Tamara; Vretenar, Dario

Source / Izvornik: **Physical Review C - Nuclear Physics, 2014, 89**

Journal article, Published version

Rad u časopisu, Objavljena verzija rada (izdavačev PDF)

<https://doi.org/10.1103/PhysRevC.89.031303>

Permanent link / Trajna poveznica: <https://um.nsk.hr/um:nbn:hr:217:193930>

Rights / Prava: [In copyright](#) / [Zaštićeno autorskim pravom.](#)

Download date / Datum preuzimanja: **2024-12-26**



Repository / Repozitorij:

[Repository of the Faculty of Science - University of Zagreb](#)



Cluster-liquid transition in finite, saturated fermionic systems

J.-P. Ebran,¹ E. Khan,² T. Nikšić,³ and D. Vretenar³

¹CEA, DAM, DIF, F-91297 Arpajon, France

²Institut de Physique Nucléaire, Université Paris-Sud, IN2P3-CNRS, F-91406 Orsay Cedex, France

³Physics Department, Faculty of Science, University of Zagreb, 10000 Zagreb, Croatia

(Received 14 November 2013; published 31 March 2014)

The role of saturation for cluster formation in atomic nuclei is analyzed by considering three length-scale ratios and performing deformation-constrained self-consistent mean-field calculations. The effect of clusterization in deformed light systems is related to the saturation property of the internucleon interaction. The formation of clusters at low nucleon density is illustrated by expanding the radius of ¹⁶O in a constrained calculation. A phase diagram shows that the formation of clusters can be interpreted as a hybrid state between the crystal and the liquid phases. In the hybrid cluster phase the confining potential attenuates the delocalization generated by the effective nuclear interaction.

DOI: [10.1103/PhysRevC.89.031303](https://doi.org/10.1103/PhysRevC.89.031303)

PACS number(s): 21.10.-k, 21.60.Jz, 21.30.Fe, 27.20.+n

When temperature decreases and density increases, a system of particles interacting through a short-range force undergoes a transition from a classical gaseous state to a liquid one. Lowering the temperature further, in most cases a first-order phase transition from the liquid state to a solid state occurs. By increasing the density, that is, adding constituents between the nodes of the microscopic crystal structure, their wave functions start to overlap and clusters can be formed. With a further increase of the density the system becomes more homogeneous, finally reaching the quantum-liquid state [1]. Quantum effects become important when the typical dispersion of the constituent particles, that is, the thermal de Broglie wavelength of a particle,

$$\lambda = \frac{h}{p} \simeq \frac{\hbar}{\sqrt{2mkT}}, \quad (1)$$

becomes comparable to the average interparticle spacing. In a transition to a quantum-liquid state the constituent particles are delocalized and the system reaches a homogeneous density. Both the bosonic/fermionic characteristic of a many-body system and the inter-particle interaction determine the properties of a quantum liquid [1].

The cluster to liquid transition in atomic nuclei characterized by a typical internucleon distance, r_0 , at saturation density can be analyzed by considering three concomitant length-scale ratios. In addition to λ/r_0 [2], where λ is given by Eq. (1), one can also consider b_0/r_0 , where

$$b_0 \simeq \frac{\hbar}{\sqrt{2mV'_0}} \quad (2)$$

and V'_0 corresponds to the typical magnitude of the interparticle interaction ($V'_0 \simeq 100$ MeV in the case of the nucleon-nucleon interaction). This ratio is related to the quantity parameter Λ introduced by Mottelson in Ref. [3]:

$$\Lambda \simeq 2 \left(\frac{b_0}{r_0} \right)^2 = \frac{\hbar^2}{mr_0^2 V'_0}. \quad (3)$$

The quantity Λ is defined as the ratio of the zero-point kinetic energy of the confined particle to its potential energy. The

liquid phase corresponds to $\Lambda > 0.1$, whereas the crystalline solid phase is characterized by values of $\Lambda < 0.1$. Finally, one can also consider the localization parameter α introduced in Ref. [4], which takes into account the finite size of the system:

$$\alpha \simeq \frac{\Delta r}{r_0} \simeq \frac{\sqrt{\hbar} A^{1/6}}{(2mV_0 r_0^2)^{1/4}}, \quad (4)$$

with Δr denoting the spatial dispersion of the single-particle wave function, A the number of constituents of the system, and V_0 the depth of the confining potential. The right-hand side of this relation corresponds to the case when the single-nucleon potential is approximated by an isotropic harmonic oscillator potential ($V_0 \simeq 75$ MeV for the nuclear mean field [4]). For $\alpha > 1$ the single-nucleon orbits are delocalized and the system is in the Fermi liquid phase. For $\alpha \sim 1$ one finds a transition from the quantum-liquid phase to a hybrid phase of cluster states [5].

The parameters defined by Eqs. (1), (3), and (4) can be used to characterize quantum phases of matter and, in particular, nuclear matter. The formation and dissociation of clusters in nuclear matter as a function of density is determined by their binding energy due to Pauli blocking that leads to the Mott effect for vanishing binding [6]. The formation of nuclear clusters is similar to a transition from a superfluid to a Mott insulator phase in a gas of ultracold atoms held in a three-dimensional optical lattice potential [7]. As the potential depth of the lattice is increased, a transition is observed from a phase in which each atom is spread out over the entire lattice to the insulating phase in which atoms are localized with no phase coherence across the lattice. In the crust of a neutron star the transition from the Wigner crystal phase to the quantum liquid also proceeds through a cluster phase as a function of density [8]. Clustering occurs as a transition between the quantum-liquid and solid-state phases because of frustration effects, that is, due to the interplay between an attractive and a repulsive interaction [9,10]. This is the case in the crust of neutron stars or for gelification in condensed matter.

The aim of this article is to analyze in more detail the role of saturation for cluster formation in finite nuclear systems.

Cluster states can occur in light nuclei and, generally, in dilute nuclear systems [6,11,12]. In light nuclei deformation can favor clustering because of a local increase in density toward its saturation value and, therefore, an increase in the binding of the system. In Ref. [5] we have shown that, contrary to the case of the crust of a neutron star, crystal-like structures cannot be formed in a nucleus. It should be noted that another possibility for the formation of nuclear clusters or even a crystal phase is to heat the nucleus. Using Eq. (1) one can estimate the temperature at which clusters form ($\lambda \sim r_0$) to be 10 MeV. This is in quantitative agreement with recent studies of critical temperatures for α -particle condensation in nuclear matter [13,14] and shows the relevance of the parameter λ/r_0 for cluster formation. Pauli blocking can be considered as a leading mechanism that suppresses clusterization at higher densities, also at finite temperatures [15]. In the present study, however, we focus on cluster formation in light nuclei, without considering effects of finite temperature.

We first consider the role of deformation in the formation of clusters and relate it to the saturation of nucleonic matter. The localization parameter (4) establishes a link between clusterization and the single-nucleon spectrum [4,5]. The relationship between α clusters and single-particle states in deformed nuclei is well known [16–18]. Rae [19] and von Oertzen *et al.* [11] have predicted that the degeneracy of single-nucleon states at a given deformation could generate clusters because of levels crossing. As already suggested by Aberg and Jönsson [18] and Freer *et al.* [20], an isolated single-particle state of the single-particle energy spectrum in a deformed self-conjugate $N = Z$ nucleus can correspond to an α cluster, due to both the Kramers (time-invariance) degeneracy and the isospin symmetry: two protons and two neutrons have similar wave functions, and the localization of these functions facilitates the formation of α clusters.

To illustrate the effect of nuclear deformation we employ the framework of deformation-constrained self-consistent mean-field calculations based on microscopic energy density functionals (EDFs). This approach has recently been successfully applied in studies of cluster phenomena in light and medium-heavy nuclei [4,5,21–26]. It has an advantage over dedicated cluster models in that it does not *a priori* assume the existence of such structures, cluster formation is described starting from microscopic single-nucleon degrees of freedom, and applications are not limited only to the lightest nuclei [26]. In fact, microscopic EDFs implicitly include many-body correlations that enable the formation of nucleon cluster structures. In Fig. 1 we display the binding energy of the self-conjugate nucleus ^{20}Ne as a function of the axial quadrupole deformation parameter β_2 . As in our previous studies of nuclear clustering [4,5], the self-consistent relativistic Hartree-Bogoliubov (RHB) model [27] has been employed in the calculation, based on the EDF DD-ME2 [28]. The curve of the total energy as a function of quadrupole deformation is obtained in a self-consistent mean-field calculation by imposing a constraint on the axial quadrupole moment. The parameter β_2 is directly proportional to the intrinsic quadrupole moment. $\beta_2 > 0$ corresponds to axial prolate shapes, whereas the shape is oblate for $\beta_2 < 0$. The calculated equilibrium shape of ^{20}Ne is a prolate,

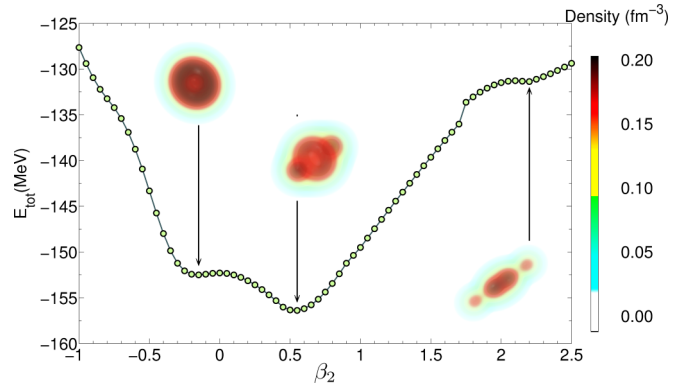


FIG. 1. (Color online) Self-consistent deformation energy curve of ^{20}Ne as a function of the quadrupole deformation parameter β_2 , calculated using the RHB model with the DD-ME2 functional. The insets display the corresponding three-dimensional intrinsic nucleon density distributions.

axially symmetric quadrupole ellipsoid with $\beta_2 \approx 0.55$, and the characteristic observables (binding energy, charge, and matter radii) reproduce the available data within 1%. For the equilibrium deformation and two additional values of β_2 , in the insets of Fig. 1 we also include the corresponding intrinsic nucleon density distributions in the reference frame defined by the principal axes of the nucleus. As noted in Refs. [4,5], the equilibrium self-consistent solution calculated with DD-ME2 yields two regions of pronounced nucleon localization at the outer ends of the symmetry axis and an oblate deformed core. Thus the intrinsic density displays a quasimolecular α - ^{12}C - α structure. The pronounced density peaks enhance the probability of formation of α clusters in excited states close to the energy threshold for α -particle emission [11,29–31]. This is clearly seen in the axial prolate density plots for values of the deformation parameter $\beta_2 > 2$, as well as in Fig. 2 where we show the self-consistent reflection-asymmetric axial intrinsic density of ^{20}Ne , calculated with DD-ME2 by imposing constraints on both the axial quadrupole and octupole

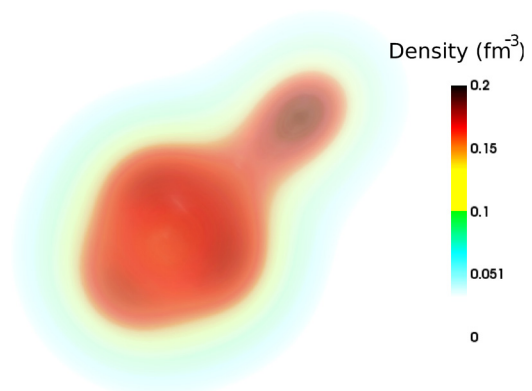


FIG. 2. (Color online) Self-consistent reflection-asymmetric axial intrinsic density of ^{20}Ne , calculated with DD-ME2 by imposing constraints on both the axial quadrupole and octupole deformation parameters. $\beta_2 = 0.55$ corresponds to the equilibrium quadrupole deformation, and $\beta_3 = 0.50$.

deformation parameters β_2 and β_3 , respectively. For these particular values of the deformation parameters ($\beta_2 = 0.55$ corresponds to the equilibrium quadrupole deformation, and $\beta_3 = 0.50$), the intrinsic density clearly presents the structure of an ^{16}O core plus the α cluster.

The intrinsic densities shown in Figs. 1 and 2 display localized latticelike structures, characteristic of the self-consistent mean-field approach that fixes the center-of-mass coordinates of α -like clusters. The RHB self-consistent solution contains the energy of the spurious center-of-mass motion of each α cluster that needs to be subtracted. A fully microscopic method for this subtraction has not been developed yet and, thus, a heuristic procedure was adopted in the analysis of Ref. [26], which yields an extra binding of ≈ 7 MeV per α particle. By restoring broken symmetries (translational, rotational, and parity in the case of octupole deformations), and allowing for configuration mixing, one would obtain solutions that correspond to nonlocalized clusters. The concept of nonlocalized clustering has recently been investigated using an angular-momentum-projected version of the Tohsaki-Horiuchi-Schuck-Röpke (THSR) wave function [32]. In light nuclei at low densities α -like clusters display a strong tendency to condense in the same orbital with respect to their center-of-mass motion [33]. Deforming the nucleus by imposing constraints on the mass multipole moments leads to excited configurations in which the single-nucleon density is reduced along the deformation axis with respect to the equilibrium. Because of the saturation property of the internucleon interaction, that is, due to the fact that the energy of nucleonic matter displays a pronounced minimum at an equilibrium density of $\rho_{\text{eq}} \approx 0.16 \text{ fm}^{-3}$, the nucleus strengthens the binding by increasing the density locally. For a relatively light nucleus, and especially for self-conjugate systems, the most effective way to increase the density locally is the formation of α clusters. This effect has very recently been investigated by Girod and Schuck [26]. By performing constrained HFB calculations of self-conjugate nuclei, with a restriction to spherically symmetric configurations, they have shown that by expanding an n - α nucleus the corresponding total energy as a function of the nuclear radius goes over a maximum before reaching the asymptotic low-density limit of a gas of α particles.

In Fig. 3 we illustrate the role saturation plays in the formation of α clusters in dilute nucleonic matter. In a self-consistent calculation similar to the one of Ref. [26] but using the relativistic functional DD-ME2, a constraint on the nuclear radius is used to gradually reduce the density of ^{16}O by inflating the spherical nucleus. As the spherical nucleus increases in size, the total energy of the system also increases with respect to the equilibrium configuration. However, when the density is reduced to $\rho/\rho_{\text{eq}} \approx 1/3$, the system undergoes a Mott-like phase transition [6,26] to a configuration of four α particles, thus locally strengthening the binding due to the saturation property of the internucleon interaction. This transition occurs at a radius of $r_c = 3.33 \text{ fm}$, as shown in Fig. 3. The corresponding ratio of the critical radius to the ground-state radius $r_c/r_{\text{g.s.}} \approx 1.3$ is smaller than the value ≈ 1.7 obtained with the Gogny effective interaction in Ref. [26]. This can be explained by the fact that single-nucleon localization in

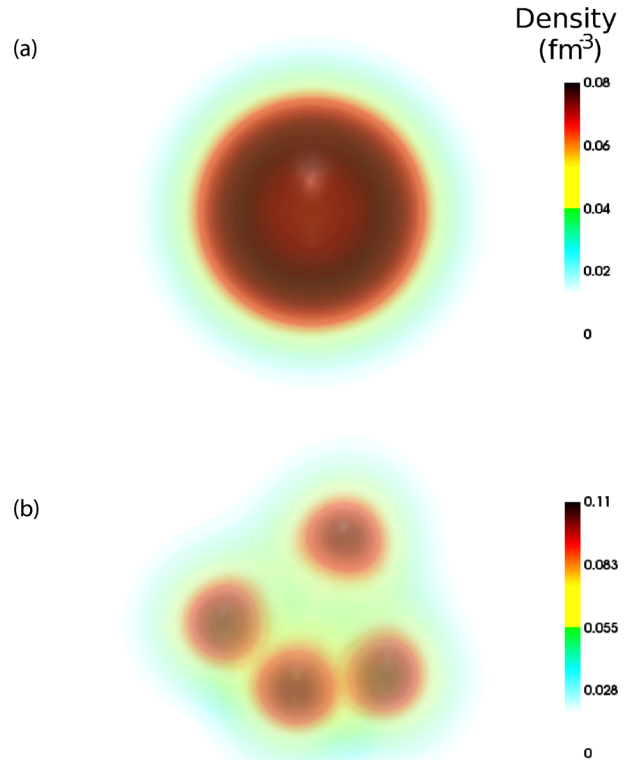


FIG. 3. (Color online) Self-consistent intrinsic nucleon density of ^{16}O for a radius constrained to 3.32 fm (a) and 3.34 fm (b).

the equilibrium intrinsic density calculated with the relativistic functional DD-ME2 is more pronounced [4,5] and, therefore, facilitates the formation of α clusters in excited states.

Saturation therefore plays a crucial role in the emergence of clusters in self-bound systems such as nuclei. In a saturated system there is a natural length scale—the equilibrium interparticle distance, which in nuclei is $r_0 \simeq 1.2 \text{ fm}$. Because of this characteristic length scale, nucleons tend to form clusters when the spatial dispersion of the single-particle wave function is of the order of r_0 . Equation (4) allows us to show that in a large nucleus the localization parameter α increases since, as it is well known, V_0 remains rather constant due to saturation. Because of the approximate $A^{1/6}$ dependence of α , medium-heavy and heavy nuclei will exhibit a quantum-liquid behavior, whereas cluster states can occur in light nuclei.

By inserting Eq. (3) into Eq. (4) one can relate the localization and quantity parameters:

$$\alpha = A^{1/6} \left(\frac{\Lambda}{2\gamma} \right)^{1/4}, \quad (5)$$

where $V_0 = \gamma V'_0$. Clustering occurs for $\alpha \simeq 1$ [5], that is, when the spatial dispersion of the single-particle wave function is of the same order as the typical interparticle distance. Inserting this last condition into Eq. (5) yields an estimate for the typical nucleon number A_0 at which one could expect clusters to occur:

$$A_0 \simeq \left(\frac{2\gamma}{\Lambda} \right)^{3/2}. \quad (6)$$

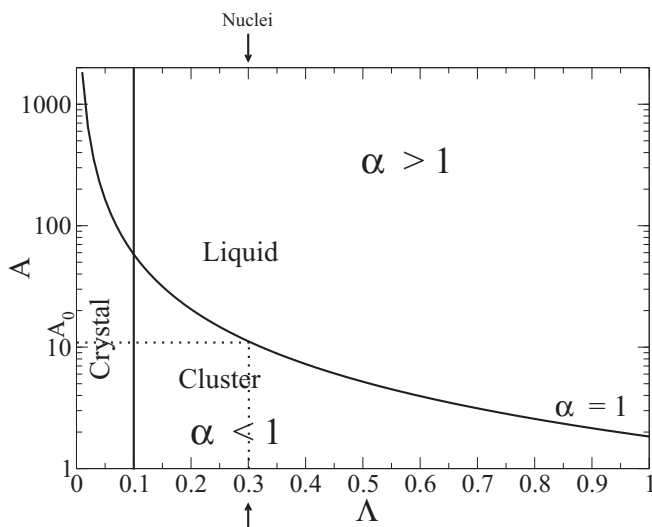


FIG. 4. Phase diagram obtained from Eq. (6), with $\gamma = 3/4$. A_0 is the nucleon number for which clustering effects are likely to occur. Λ is the quantity parameter, and the arrow denotes the typical value obtained for nuclear matter [3].

For typical values of γ in nuclei ($\gamma \sim 3/4$), and Λ in nuclear matter [3], one finds $A_0 \simeq 10$ in agreement with the mass region where cluster effects are observed [11]. Figure 4 displays the corresponding phases in finite saturated systems,

with the curve that separates the liquid and cluster phases determined by Eq. (6). This analysis supports the interpretation of clusters as a hybrid phase: for a system to behave as a liquid, Λ should be greater than 0.1 but also $A > A_0$ ($\alpha > 1$), and this underlines the importance of finite size effects in the formation of clusters. The cluster phase corresponds to $\Lambda > 0.1$ and $\alpha < 1$. In other words, the relation between α and Λ shows that in the cluster phase the confining potential attenuates the single-nucleon quantum-liquid delocalization generated by the internucleon interaction.

In summary, we have analyzed the role of saturation in the mechanism of cluster formation in finite nuclei and in dilute nuclear matter. The localization parameter describes how saturation allows for cluster and quantum-liquid phases of nuclei by relating them with the single-particle behavior through the depth of the confining potential. In deformed light nuclei the formation of clusters is favored because it locally enhances the nucleonic density toward its saturation value, thus increasing the binding of the system. In those nuclei the confining potential weakens the quantum-liquid delocalization induced by the internucleon interaction. In general, when the density of nucleonic matter is reduced below its equilibrium values, saturation causes a Mott-like transition to a hybrid phase composed of clusters of α particles.

This work was supported by the Institut Universitaire de France. The authors thank Peter Schuck for reading the manuscript and many valuable discussions.

-
- [1] D. Pines and P. Nozieres, *The Theory of Quantum Liquids* (Benjamin, Elmsford, NY, 1966).
- [2] N. T. Zinner and A. S. Jensen, *J. Phys. G: Nucl. Part. Phys.* **40**, 053101 (2013).
- [3] B. Mottelson, in *Proceedings of the Les Houches Summer School of Theoretical Physics, LXVI* (Elsevier, Amsterdam, 1996), p. 25.
- [4] J. P. Ebran, E. Khan, T. Nikšić, and D. Vretenar, *Nature (London)* **487**, 341 (2012).
- [5] J. P. Ebran, E. Khan, T. Nikšić, and D. Vretenar, *Phys. Rev. C* **87**, 044307 (2013).
- [6] S. Typel, G. Röpke, T. Klähn, D. Blaschke, and H. H. Wolter, *Phys. Rev. C* **81**, 015803 (2010).
- [7] M. Greiner, O. Mandel, T. Esslinger, T. W. Hänsch, and I. Bloch, *Nature (London)* **415**, 39 (2002).
- [8] J. M. Lattimer and F. D. Swesty, *Nucl. Phys. A* **535**, 331 (1991).
- [9] P. Napolitani, Ph. Chomaz, F. Gulminelli, and K. H. O. Hasnaoui, *Phys. Rev. Lett.* **98**, 131102 (2007).
- [10] A. Coniglio, L. De Arcangelis, A. De Candia, E. Del Gado, A. Fierro, and N. Sator, *J. Phys.: Condensed Matter* **18**, S2383 (2006).
- [11] W. von Oertzen, M. Freer, and Y. Kanada-En'yo, *Phys. Rep.* **432**, 43 (2006), and references therein.
- [12] D. M. Brink and J. J. Castro, *Nucl. Phys. A* **216**, 109 (1973).
- [13] G. Röpke, A. Schnell, P. Schuck, and P. Nozières, *Phys. Rev. Lett.* **80**, 3177 (1998).
- [14] T. Sogo, R. Lazauskas, G. Röpke, and P. Schuck, *Phys. Rev. C* **79**, 051301 (2009).
- [15] G. Röpke, *Phys. Rev. C* **79**, 014002 (2009).
- [16] Y. Kanada En'yo and H. Horiuchi, *Prog. Theor. Phys. Suppl.* **142**, 205 (2001).
- [17] H. Horiuchi, in *Clusters in Nuclei*, Vol. 1, edited by C. Beck, Lecture Notes in Physics Vol. 818 (Springer, Berlin-Heidelberg, 2010), p. 57.
- [18] S. Aberg and L.-O. Jönsson, *Z. Phys. A* **349**, 205 (1994).
- [19] W. D. M. Rae, in *Proceedings of the 5th International Conference on Clustering Aspects in Nuclear and Subnuclear Systems, Kyoto, Japan* (Physical Society of Japan, Tokyo, 1989), p. 80.
- [20] M. Freer, R. R. Betts, and A. H. Wuosmaa, *Nucl. Phys. A* **587**, 36 (1995).
- [21] P. Arumugam, B. K. Sharma, S. K. Patra, and R. K. Gupta, *Phys. Rev. C* **71**, 064308 (2005).
- [22] L. M. Robledo and G. F. Bertsch, *Phys. Rev. C* **84**, 054302 (2011).
- [23] P.-G. Reinhard, J. A. Maruhn, A. S. Umar, and V. E. Oberacker, *Phys. Rev. C* **83**, 034312 (2011).
- [24] T. Ichikawa, J. A. Maruhn, N. Itagaki, and S. Ohkubo, *Phys. Rev. Lett.* **107**, 112501 (2011).
- [25] T. Ichikawa, J. A. Maruhn, N. Itagaki, K. Matsuyanagi, P.-G. Reinhard, and S. Ohkubo, *Phys. Rev. Lett.* **109**, 232503 (2012).
- [26] M. Girod and P. Schuck, *Phys. Rev. Lett.* **111**, 132503 (2013).

- [27] D. Vretenar, A. V. Afanasjev, G. A. Lalazissis, and P. Ring, *Phys. Rep.* **409**, 101 (2005).
- [28] G. A. Lalazissis, T. Niksic, D. Vretenar, and P. Ring, *Phys. Rev. C* **71**, 024312 (2005).
- [29] K. Ikeda, N. Tagikawa, and H. Horiuchi, *Prog. Theor. Phys. E* **68**, 464 (1968).
- [30] J. Okolowicz, M. Ploszajczak, and W. Nazarewicz, *Prog. Theor. Phys. Suppl.* **196**, 230 (2012).
- [31] M. Freer, *Nature (London)* **487**, 309 (2012).
- [32] B. Zhou, Y. Funaki, H. Horiuchi, Z. Ren, G. Röpke, P. Schuck, A. Tohsaki, C. Xu, and T. Yamada, *Phys. Rev. Lett.* **110**, 262501 (2013).
- [33] T. Yamada, Y. Funaki, H. Horiuchi, G. Röpke, P. Schuck, and A. Tohsaki, in *Clusters in Nuclei*, Vol. 2, edited by C. Beck, Lecture Notes in Physics Vol. 848 (Springer, Berlin-Heidelberg, 2012), p. 229.